Materials Chemistry and Physics 145 (2014) 6–11

Contents lists available at ScienceDirect

Materials Chemistry and Physics

journal homepage: www.elsevier.com/locate/matchemphys

Materials science communication

Novel method of powder-based processing of copper nanofoams for their potential use in energy applications

Hyungyung Jo [a], Yong-Hun Cho [a,*], Myounggeun Choi [a], Jinhan Cho [b], Ji Hyun Um [c], Yung-Eun Sung [c], Heeman Choe [a]

[a] School of Advanced Materials Engineering, Kookmin University, 77 Jeongneung-ro, Seongbuk-gu, Seoul 136-702, Republic of Korea
[b] Department of Chemical and Biological Engineering, Korea University, Anam-dong, Seongbuk-gu, Seoul 136-701, Republic of Korea
[c] Center for Nanoparticle Research, Institute for Basic Science (IBS), School of Chemical and Biological Engineering, Seoul National University, Seoul 151-744, Republic of Korea

HIGHLIGHTS

- Cu nanofoams are fabricated using a simple powder-metallurgy method.
- This method is useful for producing thin Cu nanofoams with potential energy applications.
- Cu foams with multiscale pores can also be fabricated by slightly modifying the processing route.

GRAPHICAL ABSTRACT

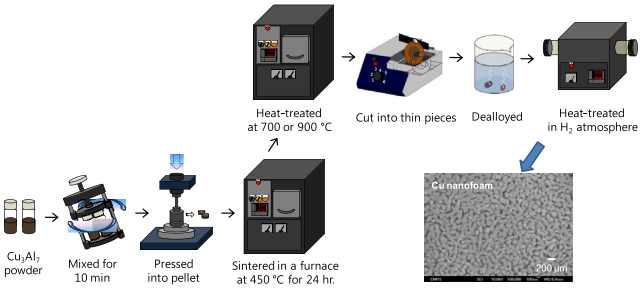

ARTICLE INFO

Article history:
Received 3 June 2013
Received in revised form
21 December 2013
Accepted 8 February 2014

Keywords:
Alloys
Intermetallic compounds
Microporous materials
Powder metallurgy
Etching

ABSTRACT

This paper discusses a new method of powder-metallurgy processing to produce regular-structured Cu nanofoams or irregular-structured Cu foams containing both micropores and nanopores. Coarser Cu nanofoam struts (approximately 2.5 times larger) formed in the ribbon samples of the foams subjected to additional sintering at 900 °C after initial lower-temperature sintering at 450 °C than those formed in the ribbon samples of the foams subjected to additional sintering at 700 °C. Furthermore, a much higher degree of strut continuity was observed in the Cu nanofoam sintered at 900 °C, which should improve the ductility and structural integrity of the Cu nanofoam. This study can be considered as a framework for using a simple method of powder-based dealloying to produce nanoporous and micro/nanoporous metallic foams for a variety of energy-based applications requiring metallic foam materials with a high density of specific surface area. Although the dealloying process of achieving Cu nanofoams is not new, this powder-based method has significant implications because often a difficult and expensive material shaping process can be avoided by forming the precursor alloy with a near-net shape geometry in the method.

1. Introduction

In order to obtain a nanoporous structure that exhibits a high density of specific surface area for energy or functional applications, a majority of earlier studies have been confined to organic or inorganic materials [1,2], because it is generally more difficult to

* Corresponding author. Tel.: +82 2 910 5672; fax: +82 2 910 4320.
E-mail address: yhun00@kookmin.ac.kr (Y.-H. Cho).

http://dx.doi.org/10.1016/j.matchemphys.2014.02.009
0254-0584/

produce a nanoporous metallic structure owing to the relatively poor oxidation and corrosion resistance of metallic materials. Despite such disadvantages, some successful attempts have recently been made to take advantage of the great potential that nanoporous metallic structures have for use in functional applications such as substrates for heat-exchanger applications, catalysts, sensors, actuators, fuel cells, and microfluidic flow controllers [3–6]; nanoporous metallic structures generally have relatively better mechanical properties and long-term operational reliability. Indeed, recent studies have focused considerable attention on processing and characterizing high-performance nanoporous noble metals through dealloying; that is, the selective dissolution during anodic corrosion in which less noble metal is dissolved out of an alloy and more noble metal remains nanoporous [7]. Moreover, since the earlier reports on nanoporous Au foams dealloyed from silver–gold alloys [8–10], there have been numerous follow-up studies on the processing, characterization, and mechanical properties of nanoporous noble metals [11,12]. For example, Chen et al. used X-ray nanotomography and microbeam diffraction to study the structural evolution of nanoporous gold produced from Ag–Au [13]; Qian and Chen produced ultrafine nanoporous Au from Ag–Au by dealloying at lower temperatures [14]; and Ateya et al. produced nanoporous Au from Cu–Au alloy [15].

The latest reports, on the other hand, have focused on methods of producing non-noble nanoporous metallic foams. For example, nanoporous Ti foams were produced using a new dealloying method based on an attractive force among the constituent elements in a metallic melt [16], nanoporous Ni foams were produced by leaching manganese in a single-phase solid solution of face-centered cubic (fcc) Ni-γMn [17], and nanoporous Cu alloy foams were produced by dealloying in an alkaline solution to extract Al from $CuAl_2$ or Cu–Al–Zn alloy systems, namely Raney copper [18–20].

The previously reported methods of producing nanoporous metallic structures are all based on complete melting processing, whereas this paper presents a novel powder-based processing method of producing the precursor alloys, which is simpler because a much lower processing temperature is required and a near-net shape geometry can be achieved directly without an additional machining or deposition process. This is important because if the nanoporous metallic foams are to be used as an electrode in batteries, die-sensitized solar cells, or fuel cells, they must be prepared in the form of a thin film with a thickness of tens to hundreds of microns; for example, anode material to be used in a typical coin cell should be a foil with a thickness of $\sim$100 μm. Therefore, use of this powder-based dealloying method makes it possible that one can avoid a difficult and costly additional material shaping process by obtaining the precursor alloy with near-net shape geometry.

In addition, this paper demonstrates that the powder-based dealloying method can be used to produce nanoscale Cu foams with the pore size on the order of a few hundreds of nanometers and can also be slightly modified to produce multiscale Cu foams containing a mixture of nanopores and micropores from Cu–Al alloys precursors.

2. Experimental

Nanoscale copper foams were synthesized using a novel powder-metallurgy process and Cu and Al powders (Cu: 99.9%, mean particle size: 1 μm, Metal Chem Tech; Al: 99.0%, mean particle size: 1 μm, Alfa Aesar, USA). A powder mixture composed of 30 at.% Cu and 70 at.% Al was blended using a simple mixing machine (8000-D Mixer Mill, SPEX CertiPrep) for approximately 10–30 min prior to compaction at room temperature. The selected composition of 30 at.% Cu and 70 at.% Al corresponds to a composition of 49.7 wt.% Cu and 50.3 wt.% Al, which is expected to yield a theoretical porosity of 76.6% on the basis of the theoretical densities of Cu and Al (Fig. 2) [21]. An air presser (DBP-6P, DONG-JIN Machine, Republic of Korea) was then used to press the powder mixture into pellets, which were subsequently sintered in an air furnace at 450 °C for 24 h. This relatively low-temperature sintering step, which was planned on the basis of the melting temperatures of Al and Cu (660 and 1085 °C, respectively, Fig. 2), was intended to serve as a 'pre-heat-treatment' process and provide a weak solid-state consolidation prior to the subsequent higher-temperature heat-treatment. One of two different follow-up processing routes was then applied to different samples of pellets in order to produce both nanoporous Cu foams and multiscale porous Cu foams containing a mixture of micropores and nanopores (Fig. 1): They are henceforth named "Cu nanofoam" and "Cu multiscale foam," respectively. For the first processing route, the pressed pellets were subjected to additional sintering at either 700 or 900 °C for 8 h to compare their microstructural features prior to dealloying in a 5 wt.% aqueous NaOH solution for 5 h. The additional higher-temperature heat-treatment was applied to ensure the achievement of a homogenous microstructure throughout the sample through the occurrence of a partial-liquid sintering, since both temperatures of 700 and 900 °C are higher than the melting temperature of Al (Fig. 2). A diamond cutting machine (Isomet low speed saw, Buehler, USA) was used to cut the specimens into thin pieces, which were subsequently polished down to a thickness of 200–250 μm in preparation for selective etching. The second processing route was as same as the first processing route until the initial low-temperature sintering at 450 °C for 24 h; however, the order of the additional higher-temperature sintering and dealloying was switched. That is, the samples were dealloyed prior to the additional higher-temperature heat-treatment (Fig. 1), which was performed at 650 °C for 2 h in a tube furnace (MSTF11-500, Myung-Sung Engineering, Republic of Korea) under H_2 atmosphere to prevent the samples from oxidizing. This final heat-treatment in H_2 atmosphere was also carried out for the sample that had been subjected to the first processing route to remove any remaining impurities. The microstructures of the Cu nanofoam and Cu multiscale foam were characterized and analyzed using scanning electron microscopy (SEM, JSM7401F, JEOL) combined with an energy dispersive X-ray spectroscopy (EDS) analyzer. X-ray diffraction (XRD, Rigaku Ultima III X-ray diffractometer) with Cu Kα radiation (λ = 1.5406 Å) was also used to determine alloy phases between Al and Cu. The mean strut size was experimentally measured using standard metallographic methods. More than ten random struts were selected on the examined fracture surface to obtain the mean strut size. For elongated struts that had an aspect ratio greater than unity, the mean size of the Cu strut was defined as the average of the largest and smallest diameters. The degree of continuity (C_S) of the Cu nanofoam strut was metallographically assessed using the contiguity parameters of N^{SS} and N^{SP}, which were determined using simple intercept measurements by drawing ten random lines of unit length on the fracture surface examined for each microstructure.

3. Results and discussion

It is generally recognized that ideal nanoporous structures can be obtained by chemically dealloying single-phase solid-solution binary alloys [18,19]. Nevertheless, to ensure a higher volume density of porosity and specific surface area, this study used a precursor alloy at a composition of 30 at.% Cu–70 at.% Al with a slightly higher Al at.% than the single-phase alloy, θ, at 33 at.% Cu–67 at.% Al [21]. It is possible to dealloy Al out of the Al–Cu system because of the large difference in the standard potentials of Al and Cu (−1.662 V *vs.* standard hydrogen electrode (SHE) for Al/Al^{3+} and

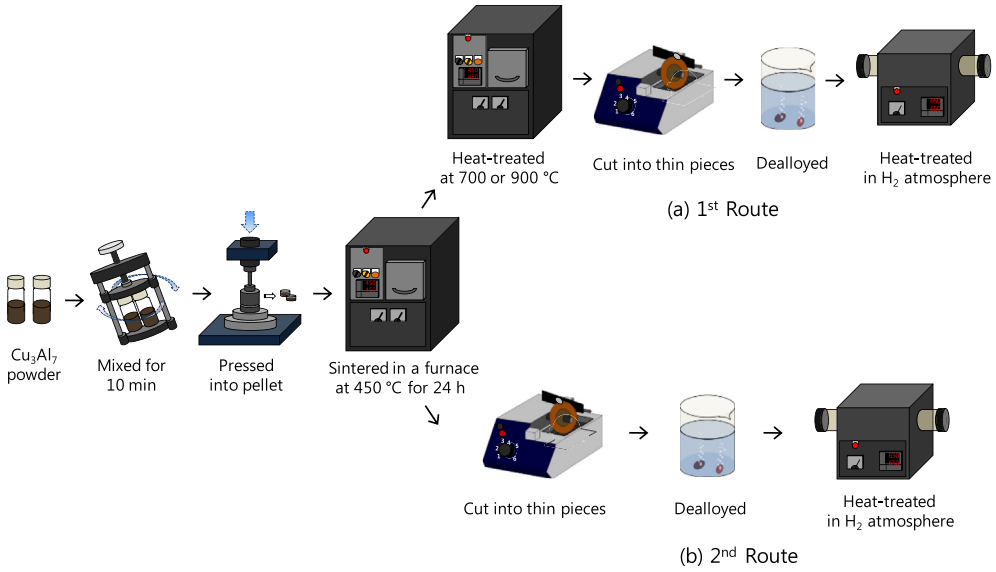

Fig. 1. Schematic illustration showing two different experimental procedures for producing (a) nanoporous (1st route) and (b) nanoporous/microporous (2nd route) Cu foam samples.

0.342 V *vs.* SHE for Cu/Cu^{+2} [18]). In addition, this dealloying is particularly easy because Al cannot only be etched in an acidic solution but also be etched in an alkaline solution since Al is amphoteric; this study used a 20 wt.% aqueous NaOH solution at ambient temperature for selective etching.

Fig. 3 compares the XRD patterns of samples after sintering in air at 450 °C for 24 h (Fig. 3(a)) and after an additional sintering at 700 °C for 8 h (Fig. 3(b)). With sintering at the relatively lower temperature of 450 °C, diffusion of Al and Cu atoms is not sufficiently fast to make the Al–Cu mixture to form single uniform phase of Al_2Cu phase. Instead, fairly intense peaks of Cu, Al, and $Al_2Cu_{3.4}$ are also observed, suggesting that those phases are present along with the thermodynamically favorable Al_2Cu phase at this stage. On the other hand, the Al–Cu powder mixture shows XRD peaks only due to Al_2Cu and Al after the additional sintering at 700 °C for 8 h (Fig. 3(b)). The weak XRD peaks of Al are due to the initial atomic ratio of Al to Cu being intentionally set at 7:3, resulting in a small excess of Al after complete consumption of Cu phase in forming single-phase Al_2Cu intermetallic compound. Peaks corresponding to any other intermetallic compounds such as AlCu, Al_2Cu_3, Al_3Cu_4, and Al_4Cu_9 are not seen at this stage, because the additional sintering at 700 °C could allow the sufficiently fast diffusion process of Al above its melting temperature. The mean crystallite size of Al_2Cu phase was estimated and compared between each of the two sintering steps using the Scherrer formula. The mean crystallite sizes of Al_2Cu phase were calculated to be 25.4 ± 0.2 nm and 26.0 ± 0.2 nm for the samples after sintering at 450 °C and an additional sintering at 700 °C, respectively. As expected, the mean crystallite size of Al_2Cu phase increased slightly with increasing time and temperature of heat-treatment, despite the statistically insignificant difference between those two mean values.

Fig. 4 compares the microstructures of the Cu nanofoams produced using the first processing route that is subjected to additional sintering at either 700 (Fig. 4(a) and (b)) or 900 °C (Fig. 4(c) and (d)) for 8 h. In addition, all Cu foam ribbons were analyzed using EDS, and one representative spectrum is shown in the inset of Fig. 4(a), indicating that Al had been completely removed during dealloying. We have thus used image analysis to estimate the porosities of the samples obtained after each of the two different sintering

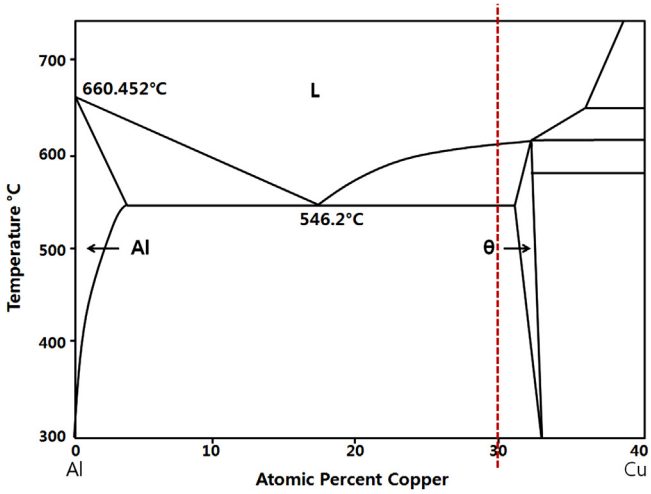

Fig. 2. Cu–Al binary phase diagram [21].

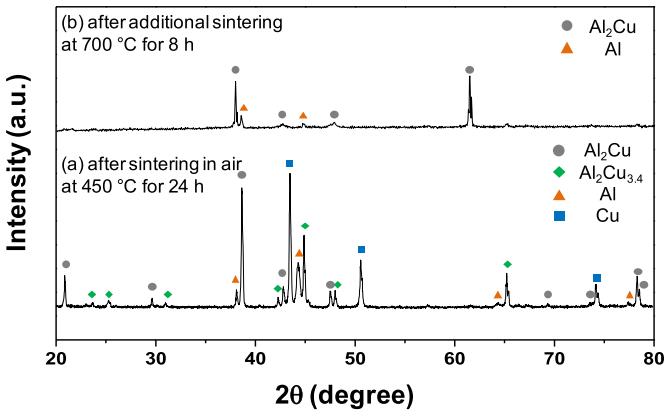

Fig. 3. XRD patterns of a simple mixture (30 min) of 30 at.% Cu–70 at.% Al precursor powder (a) after the first sintering in an air furnace at 450 °C for 24 h and (b) after the second sintering at 700 °C for 8 h.

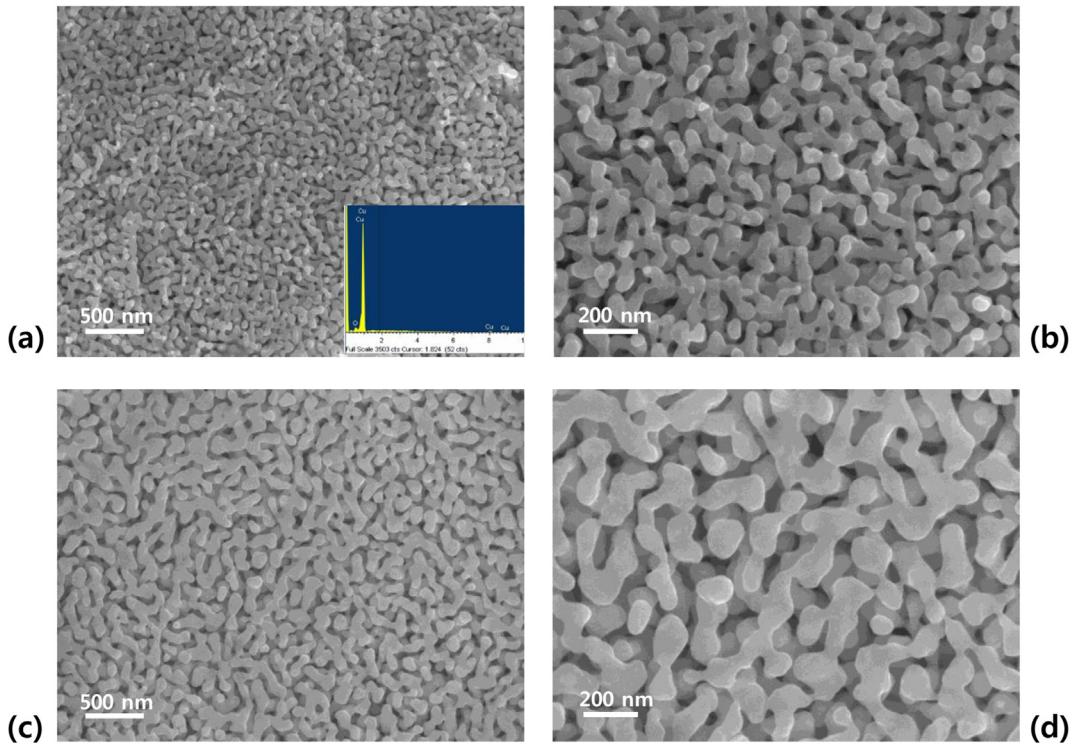

Fig. 4. SEM images of fracture surface showing nanoporous copper exhibiting three-dimensionally interconnected nanoligaments produced by dealloying mixture of 30 wt.% Cu and 70 wt.% Al powder. Two-step sintering was performed prior to dealloying: first at 450 °C and then either at 700 °C ((a) and (b)) or at 900 °C ((c) and (d)) to compare evolution of microstructures. Inset of (a) shows typical EDX spectrum for random spot selected in Cu nanofoam, indicating that Al was completely removed during dealloying.

processes at the temperatures of 700 and 900 °C. The porosities were estimated to be 57.5 ± 0.03 and 56.1 ± 0.86 for the dealloyed samples after each of the additional heat-treatment at 700 °C and 900 °C, respectively. These measured porosity values are assumed to be lower than the actual values, because of the uncertainties associated with the image analysis method performed in two dimensions. It is concluded that the two Cu foam samples have similar porosities within error range. In contrast, the two Cu foams showed different strut dimensions with the similar high-aspect-ratio strut morphology. In other words, despite the foams having the same composition of 30 at.% Cu and 70 at.% Al, the dimensions of the pore and strut varied significantly because they depend on the applied sintering temperature. The mean strut size was 92 ± 17 nm for the Cu nanofoam subjected to additional sintering at 700 °C whereas it was 228 ± 35 nm for the Cu nanofoam subjected to additional sintering at 900 °C, which is approximately 2.5 times larger. This result suggests that the Cu nanofoam sintered at a lower temperature of 700 °C should have a higher density of specific surface area, and hence, should be more beneficial for catalytic reaction applications. Although the mean strut size for the Cu nanofoam sintered at 900 °C was much larger than that for the Cu nanofoam sintered at 700 °C, it is nonetheless reasonable because the strut and pore sizes should increase with increasing heat-treatment temperature. The typical diffusion distance, d, can be estimated using Einstein's expression:

$$d \approx \sqrt{2Dt} \tag{1}$$

where the sintering time, t, is 8 h, and the diffusion coefficient, $D = D_o \exp(-Q/RT)$ is calculated as 5.804×10^{-9} and 3.898×10^{-8} m^2 s^{-1} from the data for the diffusion of Cu in liquid Al, as listed in Ref. [22]. The pre-exponential factor, D_o, is taken as 1.1×10^{-7} and 2.1×10^{-7} m^2 s^{-1}, the activation energy, Q, is taken as 23.8 and 16.5 kJ mol^{-1}, and the absolute temperature, T, is taken as 973 and 1173 K for the Cu nanofoams sintered at 700 and 900 °C, respectively. The gas constant, R, is 8.3144 J mol^{-1} K^{-1}. On the basis of approximation (1), the calculated ratio of the mean strut diameters for the Cu nanofoams sintered at 700 and 900 °C, $d_1/d_2 \sim 0.40$ is consistent with the ratio of the estimated diffusion distances of Cu in liquid Al, $d_1/d_2 \sim 0.39$, suggesting that it might be possible to assume that the strut diameter is roughly linearly proportional to the diffusion distance of Cu in liquid Al during sintering of the Cu–Al alloy system.

However, it is also possible to take advantage of the coarsening of the Cu nanofoam sintered at 900 °C because the coarsening might decrease the brittleness commonly associated with metallic nanofoams, as reported elsewhere [23]. This should also be taken into account since some degree of mechanical integrity, including ductility and strength, is still required for them to be used as an electrode in energy applications. On the basis that the coarsening accompanies a higher degree of strut connectivity (Fig. 4), the degree of strut continuity was estimated and compared for the Cu nanofoams sintered at 700 and 900 °C by measuring the contiguity, C_S, following Fan's approach in Refs. [24,25] as follows:

$$C_S \approx \frac{2N^{SS}}{2N^{SS} + N^{SP}}, \tag{2}$$

where N^{SS} and N^{SP} are the numbers of intercepts of the strut/strut and strut/pore interfaces, respectively, within a random line of unit length on the examined fracture surfaces shown in Fig. 4(b) and (d). Although the strut structure in the Cu nanofoam sintered at 700 °C is relatively discontinuous ($C_S \sim 0.3$, Fig. 4(b)), the strut structure in the Cu nanofoam sintered at 900 °C is somewhat semicontinuous ($C_S \sim 0.4$, Fig. 4(d)), implying that higher-temperature sintering at 900 °C can be more beneficial for improving the ductility of the Cu

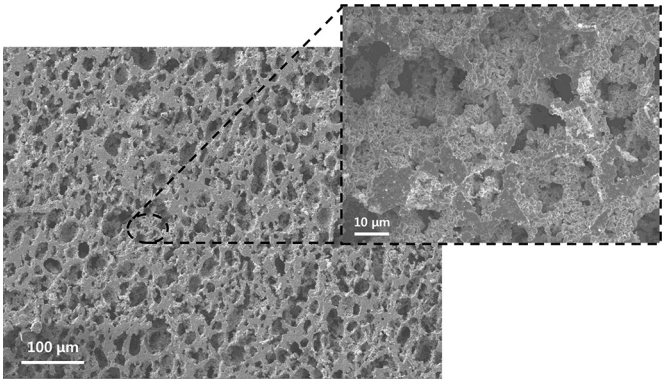

Fig. 5. Cross-sectional SEM image of dealloyed powder mixture consisting of 30 wt.% Cu and 70 wt.% Al powder. This sample was produced using the second processing route: lower-temperature sintering, dealloying, and then additional high-temperature heat-treatment. Both micropores and nanopores are present in this microstructure.

nanofoam by increasing the continuity of the structure of the Cu struts.

Fig. 5 shows the microstructure in the fracture surface of a ribbon sample produced using the second processing route. A nonuniform porous structure consisting of microsized and nanosized pores is observed. Nanopores are shown in the magnified micrograph on the right, and a few orders of magnitude larger micropores are randomly distributed at a relatively high frequency throughout the specimen, as shown in the micrograph on the left. The presence of micropores clearly indicates that Al–Cu could not be mixed and alloyed completely at the low sintering temperature of 450 °C; the subsequent elimination of agglomerated Al powder particles in the alkaline solution created those micropores. The nanosized pores, on the other hand, are the result of relatively well-mixed and alloyed portions in the ribbon sample.

Although the regular structure of the Cu nanofoams produced using the first processing route suggests that the Cu nanofoams have potential for application as anodes in high-performance lithium-ion batteries after the Cu nanofoams are coated with an "active" material such as tin [26], the irregular microporous/nanoporous structure of the Cu multiscale foam produced using the second processing route suggests that the Cu multiscale foam should also have great potential for application as either a gas diffusion layer (GDL) or an electrode in polymer electrolyte membrane fuel cells (PEMFCs) [27]. This is because the presence of micropores and nanopores can help improve the flows of water and gas, and the transfer of electrons, respectively.

In this study, Cu_3Al_7 alloy was used as a model material for introducing a novel method of powder-based dealloying. The choice of material should not be limited but should be open to other candidate metallic materials (such as titanium, nickel, and so forth) that meet the conditions required for specific applications. This study can be considered as a framework for using a simple method of powder-based dealloying to produce nanoporous or microporous/nanoporous metallic foams because the experimental procedure and insights obtained from the results presented here may also apply to processing other non-noble nanoporous metals for a variety of energy-based applications.

4. Conclusions

On the basis of the results of this study, the following conclusions can be made:

1. A simple method of powder-metallurgy processing was used to produce Cu nanofoams that exhibited strut sizes on the order of several tens to hundreds nanometers. A uniform nanoporous structure was observed throughout the thickness of the specimen. Compared to the struts formed in the Cu nanofoam sintered at 700 °C, the coarser struts formed in the Cu nanofoam sintered at 900 °C lose a certain portion of their specific surface area, also forming larger pores between the struts. This however increased the strut connectivity, as estimated by measuring the contiguity (C_S), and is expected to result in better ductility and integrity of the Cu nanofoam.
2. In addition, a nonuniform porous structure consisting of both microsized and nanosized pores was produced by slightly modifying the powder-based processing route; that is, dealloying was performed immediately after the low-temperature sintering at 450 °C prior to additional high-temperature heat-treatment. Much larger micropores were randomly distributed at a relatively high frequency throughout the specimen, which clearly indicates that Al–Cu cannot be completely mixed and alloyed at the low sintering temperature of 450 °C. Conversely, the presence of nanopores can be interpreted as the result of well-mixed and alloyed regions in the ribbon sample.
3. Both types of porous structures, the regular nanoporous structure and irregular porous structure consisting of a mixture of micropores/nanopores, can be used as catalytic electrode materials in various energy-based applications. The regular-structured Cu nanofoams have potential for application as anodes in high-performance lithium-ion batteries, and the irregular-structured Cu microfoam/nanofoam has potential for application as either a GDL or an electrode in PEMFCs. The concurrent presence of micropores and nanopores is expected to improve the flows of water and gas, and the transfer of electrons, respectively.

Acknowledgments

This research was supported by the Pioneer Research Center Program through the National Research Foundation (NRF) of Korea funded by the Ministry of Education, Science, and Technology (2011-0001684). HC also acknowledges support from the Basic Science Research Program (2010-0005775) and the Priority Research Centers Program (2009-0093814; 2010-0029106) through the National Research Foundation (NRF) of Korea funded by the Ministry of Education, Science, and Technology. YS also acknowledges support from the Institute for Basic Science (IBS).

References

[1] J.Y. Lee, K.H. Ju, Y.M. Yi, J.M. Lee, S.H. Uhm, J.K. Lee, H.J. Lee, J. Phys. Chem. C. 116 (2012) 2915–2918.
[2] Z.H. Zhang, C. Zhang, J. Sun, T. Kou, C.C. Zhao, RSC Adv. 2 (2012) 11820–11828.
[3] G.C. Bond, D.T. Thompson, Catal. Rev. Sci. Eng. 41 (1990) 319–388.
[4] J. Biener, A. Wittstock, L.A. Zepeda-Ruiz, M.M. Biener, V. Zielasek, D. Kramer, R.N. Swanath, J. Weissmüller, M. Baümerand, A.V. Hamza, Nat. Mater. 8 (2009) 47–51.
[5] H.J. Jin, X.L. Wang, S. Parida, K. Wang, M. Seo, J. Weissmüller, Nano Lett. 10 (2010) 187–194.
[6] R. Wang, C. Wang, W. Cai, Y. Ding, Adv. Mater. 22 (2010) 1845–1848.
[7] A.J. Forty, Nature 282 (1979) 597–598.
[8] X. Lu, T.J. Balk, R. Spolenak, E. Arzt, Thin Solid Films 515 (2007) 7122–7126.
[9] A.M. Hodge, J. Biener, L.L. Hsiung, A.V. Hamza, J.H. Satcher, J. Mater. Res. 20 (2005) 554–557.
[10] J. Erlebacher, M.J. Aziz, A. Karma, N. Dimitrov, K. Sieradzki, Nature 410 (2001) 450–453.
[11] J. Biener, A.M. Hodge, A.V. Hamza, L.M. Hsiung, J.H. Satcher, J. Appl. Phys. 97 (2005) 024301.
[12] D.G. Lee, X. Wei, X. Chen, M.H. Zhao, S.C. Jun, J. Hone, E.G. Herbert, W.C. Oliver, J.W. Kysar, Scr. Mater. 56 (2007) 437–440.
[13] Y.K. Chen-Wiegart, S. Wang, Y.S. Chu, W. Liu, I. McNulty, P.W. Voorhees, D.C. Dunand, Acta Mater. 60 (2012) 4972–4981.
[14] L.H. Qian, M.W. Chen, Appl. Phys. Lett. 91 (2007) 83105.
[15] B.G. Ateya, J.D. Fritz, H.W. Pickering, J. Electrochem. Soc. 144 (1997) 2606–2613.

[16] T. Wada, K. Yubuta, A. Inoue, H. Kato, Mater. Lett. 65 (2011) 1076–1078.
[17] M. Hakamada, Y. Chino, M. Mabuchi, J. Alloys Compd. 485 (2009) 583–587.
[18] Z. Qi, C. Zhao, X. Wang, J. Lin, W. Shao, Z. Zhang, X. Bian, J. Phys. Chem. C. 113 (2009) 6694–6698.
[19] W.B. Liu, S.C. Zhang, N. Li, J.W. Zheng, Y.L. Xing, Corros. Sci. 53 (2011) 809–814.
[20] A.J. Smith, D.L. Trimm, Annu. Rev. Mater. Res. 35 (2005) 127–142.
[21] E.A. Brandes, G.B. Brook, Smithells Metals Reference Book, seventh ed., Butterworth–Heinemann, Oxford, 1998.
[22] Y. Du, Y.A. Chang, B. Huang, W. Gong, Z. Jin, H. Xu, Z. Yuan, Y. Liu, Y. He, F.Y. Xie, Mater. Sci. Eng. A 363 (2003) 140–151.
[23] J. Biener, A.M. Hodge, J.R. Hayes, C.A. Volkert, L.A. Zepeda-Ruiz, A.V. Hamza, F.F. Abraham, Nano Lett. 6 (2006) 2379–2382.
[24] J. Gurland, Trans. Met. Soc. AIME 212 (1958) 452–455.
[25] Z. Fan, A.P. Miodownik, P. Tsakiropoulos, Mater. Sci. Technol. 9 (1993) 1094–1100.
[26] Z. Du, S. Zhang, T. Jiang, Z. Bai, Electrochim. Acta 65 (2010) 3537–3541.
[27] O. Kim, Y. Cho, S. Kang, H. Park, M. Kim, J. Lim, D. Chung, M. Lee, H. Choe, Y. Sung, Nat. Commun. 4 (2013) 2473.